sustainability

MDPI

Article

Assessing the Reliability of Thermal and Optical Imaging Techniques for Detecting Crop Water Status under Different Nitrogen Levels

Daniele Masseroni *, Bianca Ortuani, Martina Corti, Pietro Marino Gallina, Giacomo Cocetta, Antonio Ferrante and Arianna Facchi

Department of Agricultural and Environmental Sciences (DiSAA), Università degli Studi di Milano, Via Celoria 2, 20133 Milan, Italy; bianca.ortuani@unimi.it (B.O.); martina.corti@unimi.it (M.C.); pietro.marino@unimi.it (P.M.G.); giacomo.cocetta@unimi.it (G.C.); antonio.ferrante@unimi.it (A.Fe.); arianna.facchi@unimi.it (A.Fa.)

* Correspondence: daniele.masseroni@unimi.it; Tel.: +39-02-503-16903; Fax: +39-02-503-16911

Received: 10 May 2017; Accepted: 22 August 2017; Published: 30 August 2017

Abstract: Efficient management of irrigation water is fundamental in agriculture to reduce the environmental impacts and to increase the sustainability of crop production. The availability of adequate tools and methodologies to easily identify the crop water status in operating conditions is therefore crucial. This work aimed to assess the reliability of indices derived from imaging techniques—thermal indices (I_g (stomatal conductance index) and *CWSI* (Crop Water Stress Index)) and optical indices (*NDVI* (Normalized Difference Vegetation Index) and *PRI* (Photochemical Reflectance Index))—as operational tools to detect the crop water status, regardless the eventual presence of nitrogen stress. In particular, two separate experiments were carried out in a greenhouse, on two spinach varieties (Verdi F1 and SV2157VB), with different microclimatic conditions and under different levels of water and nitrogen application. Statistical analysis based on ANOVA test was carried out to assess the independence of thermal and optical indices from the crop nitrogen status. These imaging indices were successively compared through correlation analysis with reference destructive and non-destructive measurements of crop water status (stomatal conductance, chlorophyll *a* fluorescence, and leaf and soil water content), and linear regression models of thermal and optical indices versus reference measurements were calibrated. All models were significant (Fisher *p*-value lower than 0.05), and the highest R^2 values (greater than 0.6) were found for the regression models between *CWSI* and the soil water content, *NDVI* and the leaf water content, and *PRI* and the stomatal conductance. Further analysis showed that imaging indices acquired by thermal cameras (especially *CWSI*) can be used as operational tools to detect the crop water status, since no dependence on plant nitrogen conditions was observed, even when the soil water depletion was very limited. Our results confirmed that imaging indices such as *CWSI*, *NDVI* and *PRI* can be used as operational tools to predict soil water status and to detect drought stress under different soil nitrogen conditions.

Keywords: optical imaging sensor; thermal camera; spectral imaging index; crop water status; crop water stress prediction

1. Introduction

The knowledge of crop water status plays a role in many applications within biophysical, natural and agricultural research fields. When agricultural research is taken into account, water stress is one of the most important factors limiting the primary production and thus the quantitative yield [1]. An accurate knowledge of the crop water status can help farmers to manage irrigation in a more

efficient way, reducing the water losses and the potential mobilization of nutrients and pesticides to surface water and groundwater [2–4]. Visible-near infrared and thermal spectral sensing techniques can be seen as useful tools to assess plant status rapidly and accurately, without the need for destructive measurements and time-consuming analytical determinations. In particular, different eco-physiological variables involved in plant water use processes can be investigated using thermal cameras that acquire data in the Thermal InfraRed (TIR) region of the electromagnetic spectrum [5,6]. Indeed, a soil water deficit causes a reduction in root water uptake and plant transpiration, and an increase of canopy temperature. Research on thermal imaging started a few decades ago [7] and, since then, many studies aimed to assess the crop water status by means of thermal images have been developed [8–10]. The most used crop water stress index based on thermal data is the Crop Water Stress Index (*CWSI*), where the temperature difference between well-watered and dry canopy is normalized using a proxy of the evaporating power of the air above the crop [11]. Another widely adopted index based on thermal data is the stomatal conductance index (I_g), originally proposed by Jones [12], whose value should be directly related to the stomatal conductance (g_s).

Although many studies demonstrated that thermal data is successful in detecting crop water stress, several attempts have been also made to retrieve crop water status from reflectance data collected in the Visible-Near InfraRed (VIS-NIR) regions of the spectrum by using optical sensors. Contrasting results were obtained, especially concerning the ability of the optical indices (e.g., Normalized Difference Vegetation Index (*NDVI*) and Photochemical Reflectance Index (*PRI*)) to identify the nature of different crop stresses [13,14]. This is a relevant issue; indeed, different stressors may induce similar effects on the canopy optical properties in the VIS-NIR region [15]. Some authors pointed out how spectral measurements may record confounding effects in detecting nitrogen stress under water limiting conditions and vice versa [16]. Water stress is known to change the spectral effects of the nutrient deficiencies and it can reduce, or remove, specific spectral properties related to nitrogen stress [17], e.g., lowering of the red light absorbance. Nitrogen availability can be associated with the greenness of leaves [18], due to the relationship of the chlorophyll content (in particular chlorophyll *a*) with the leaf nitrogen content; the chlorophyll content also affects the photosynthesis activity and the leaf gas exchanges. Nevertheless, both soil moisture depletion and low nitrogen availability can drive confounding effects on the canopy optical properties, possibly due to changes in canopy architecture, to reflectance coming from the bare soil as well as to changes in the properties of leaves surfaces [19].

Since crops may undergo different stresses (e.g., nitrogen and water stresses), it may be crucial to find and select diagnostic tools that are more sensitive to each specific stress type to enable the development of operational decision support systems which can help the grower to manage water and chemical inputs.

In greenhouse experiments, many variables governing the crop growth can be controlled, and different scenarios of crop water and/or nutrient status can be configured and investigated. In fact, it is possible to control the hydraulic proprieties of soil by choosing the substrate, select the optimal sowing density, and adjust the microclimate by means of automatic cooling, heating, and lighting systems. Moreover, water and nutrients applications may be scheduled, and soil water content and plant nitrogen status may be accurately monitored. All these factors contribute to make the greenhouse an optimal environment to investigate the effect of different types of stresses on spectral indices, and to check which indices are better suited to detect a certain type of stress [20]. However, greenhouse experiments may have some limits in different seasons, such as low light intensity during winter, and a general tendency to high air relative humidity (low vapor pressure deficit (VPD)) which limits leaf gas exchange. For this reason, an optimal climate control should be adopted to maintain all the environmental parameters in proper ranges in spite of the season.

This study focuses on the evaluation of the ability of thermal and optical imaging sensing applied to a spinach crop cultivated in greenhouse to detect crop water status under different nitrogen application levels. Two experiments were setup with two varieties of spinach in two different periods of the year. Statistical analysis based on the ANOVA test was carried out to assess the independence of

thermal and optical imaging indices from crop nitrogen status. Afterwards, the thermal and optical indices were compared with direct measurements of crop water status, obtained through destructive and non-destructive techniques. Finally, correlation analysis and linear regressions between thermal and optical indices and reference measurements were conducted to evaluate the ability of spectral indices to monitor the crop water status and predict the crop water stress.

2. Materials and Methods

2.1. Experimental Setup

Two experimental campaigns were carried out on two different spinach (*Spinacia oleracea* L.) cultivars grown in pots into a greenhouse of the Department of Agricultural and Environmental Sciences at the University of Milan (Figure 1). In particular, in Experiment 1 (EX1), the spinach cultivar Verdi F1 (ISI Sementi S.p.A., Fidenza, Italy), suitable for early-spring greenhouse growing, was selected. During Experiment 2 (EX2), the SV2157VB cultivar (Seminis Seeds Vegetables) was grown due to its suitability for spring–summer greenhouse production. The two cultivars have similar developmental stages and canopy structure. The sowing dates were 28 January and 18 April, while the germination dates were 4 February and 24 April, for the first and second cultivars respectively. The harvesting dates were 20 March and 24 May, respectively, for the two cultivars.

(**a**) (**b**)

Figure 1. (**a**) Greenhouse external structure; and (**b**) disposition of counters, pots, lighting and cooling systems.

The greenhouse is equipped with heating and cooling systems, as well as a lighting system with 28 High-Pressure Sodium (HPS) lamps emitting a light energy of about 400 W m^{-2} (1990 µmol m^{-2} s^{-1}) in the wavelength range 400–700 nm. An artificial photoperiod of about 16 h of light and 8 h of darkness was setup during EX1 (from 14 March to 20 March), while the natural photoperiod (about 12 h of light and 12 of darkness) was setup during EX2 (from 18 May to 24 May). An integrated system to measure the agro-meteorological variables inside and outside the greenhouse structure was used to automatically manage the indoor microclimate by means of the heating/cooling control system. In particular, measurements of air temperature, humidity and global radiation were registered by two Davis Vantage Pro2 stations (one inside and the other outside the greenhouse placed on the roof). Moreover, outside the greenhouse, wind velocity and direction are also measured by a digital cup anemometer (Davis Instruments, Hayward, CA, USA).

The substrate of each pot (10 L of volume) consisted of 50% of silica sand with neutral reaction (particles size 0.4–0.8 mm), and 50% of soil (sieved at 5 mm). An optimal amount of macro and micro-nutrients (28 kg ha^{-1} of P_2O_5, 118 kg ha^{-1} of K_2O, 9 kg ha^{-1} of Mg and 1 kg ha^{-1} of a balanced mixture of micro-nutrients) was mixed with the substrate. The final substrate had the following

characteristics: 52% sand, 39% silt, 9% clay, pH (water) 7.4, pH (KCl) 6.6, total nitrogen content 0.13%, total carbon 1.4%, nitrogen nitric 11.28 ppm, ammonia nitrogen 3.63 ppm, and bulk density 1.28 g cm^{-3}. The substrate volumetric water content at the field capacity (−10 kPa) and at the wilting point (−1500 kPa), as determined by a Richards' apparatus over soil samples collected in three different pots, was found to be respectively 0.14 m^3 m^{-3} and 0.05 m^3 m^{-3}. A layer of 5 cm of expanded clay was placed on the bottom of the pots, whereas a thin filter fabric with fine mesh was placed between the substrate and the expanded clay to limit the drainage flow on the bottom of the pots and to separate the two materials (i.e., substrate and expanded clay).

Four different levels of nitrogen (N0, N1, N2, and N3) were considered: (i) N0 was the not fertilized treatment in both experiments; (ii) N1 was obtained in both experiments by decreasing of 50% the nitrogen level set for N2; (iii) N2 in EX1 corresponded to the optimal level of nitrogen application (66 kg N ha^{-1}), as obtained from the generalized equation for the C3 cultivars [21], while N2 in EX2 corresponded to a doubled nitrogen rate with respect to the value calculated for EX1 (132 kg N ha^{-1}): the increased nitrogen level was applied in EX2 to achieve more marked effects on the crop nitrogen status; and (iv) N3 was obtained in both experiments by increasing of 50% the nitrogen level set for N2. Different numbers of pots were involved in the experiments: (i) N0: 2 pots in EX1 and 9 pots in EX2; (ii) N1: 4 pots in EX1 and 9 pots in EX2; (iii) N2: 2 pots in EX1 and 9 pots in EX2; and (iv) N3: 4 pots in EX1 and 19 pots in EX2.

The four nitrogen levels were combined with two irrigation treatments (W+, and W−): (i) W+ considered optimal amount of water in both experiments (6 pots in EX1 and 16 pots in EX2); and (ii) W− was obtained in both experiments with no water applied from a certain specific date until the death of plants (6 pots in EX1 and 20 pots in EX2) to induce a water stress from mild to very severe. For the treatment W+, pots were maintained in well-watered conditions, replacing daily the water lost by evapotranspiration. The water replacement was performed by weighing each pot every day (using a weighing balance with an accuracy of ±1 g), and replenishing the soil water content to the field capacity value. Soil water content never dropped below the RAW (Readily Available Water), assumed equal to 20% of the TAW (Total Available Water, defined as the difference between volumetric water content at field capacity and wilting point), as reported in Allen et al. [22] for spinach crop. For treatment W−, the water replacement was interrupted from 14 March for EX1, and from 18 May for EX2. More information about the setup of the experiments are reported in [4]. In Table 1, this information is briefly summarized.

Due to the differences in the spinach cultivars grown, in the greenhouse microclimatic conditions, and in the nitrogen rates applied, the two experimental campaigns cannot be considered as replicates, but they must be considered as independent experiments carried out on the same crop species.

Table 1. Number of pots for the various combinations of nitrogen and irrigation treatments.

Experimental Campaign (EX)	Cultivar	Sowing Date	Harvesting Date	Sowing Density (Plant/m^2)	Start Survey	End Survey	Irrigation Treatment	Number of Pots				Total Number of Pots
								N0	N1	N2	N3	
1	Verdi F1	28 January	20 March	100	14 March	20 March	W+	1	2	1	2	12
							W−	1	2	1	2	
2	SV2157VB	18 April	24 May	200	18 May	24 May	W+	2	2	2	2	36
							W−	3	3	3	3	
							W+	2	2	2	2	
							W−	2	2	2	2	

2.2. Reference Measurements to Assess the Crop Water Status

The thermal and optical imaging indices were compared with reference measurements known from the literature to be suitable for crop water stress assessment, both non-destructive (volumetric soil water content, stomatal conductance and chlorophyll *a* fluorescence) and destructive (water content of aerial biomass). The reference measurements used in this study are summarized in Appendix A. In EX1, only non-destructive measurements were performed, while in EX2 the pots were split in two groups, separately intended for non-destructive and destructive measurements.

The volumetric soil water content (*VWC*) is directly related to the amount of water available for plant uptake. For each pot, the volumetric water content of the soil at time t (VWC_t) was calculated from daily measurements of the pot weight, according to the following equation:

$$VWC_t = \frac{P_t \cdot VWC_{t_0}}{P_{t_0}} \quad (1)$$

where VWC_{t0} is the volumetric water content at field capacity, P_{t0} is the weight of the pot at field capacity (equal to 23.6 kg), and P_t is the weight of the pot measured at time t.

The stomatal conductance (g_s) is a key variable in plants for photosynthesis and transpiration. It was used as a reference measure of crop water status, according to Moller et al. [23]. It was measured by a LICOR-1600 porometer (LICOR Industry, Lincoln, NE, USA) on the 5th–6th leaf of spinach plants, since this stage is of interest for the fresh cut market. At this stage, leaves were fully developed and with the optimal photosynthetic potential. The opening of the cuvette was set to 2 cm^2. The g_s value for each pot was obtained as the mean value of three-four measurements on leaves of different plants [24]. The g_s measurements were conducted immediately after thermal and optical acquisitions, to avoid that the porometer's clamp could significantly affect the leaf temperature.

In abiotic stress studies (e.g., drought and nitrogen deficiency), the chlorophyll *a* fluorescence and the derived indices have been successfully used to assess the plant stress conditions [25–27]. In this study, chlorophyll *a* fluorescence was measured with the portable fluorometer "Handy-PEA" (Hansatech, Norfolk, UK). Prior to the assay, the leaves were kept in the dark for 30 min in order to remove all electrons from the photosystem II [28,29]. Measurements were then taken on the leaf surface (4 mm diameter) exposed to an excitation light intensity (ultra-bright red light emitting devices (LEDs) with a peak at 650 nm) of 3000 µmol m^2 s^{-1} (600 W m^2) emitted by three diodes. Fluorescence detection was measured by fast response PIN photodiode with RG9 long pass filter. From the fluorescence measurements, the following indices were calculated, according to Guidi and Calatayud [30]: the ratio between the value of variable fluorescence (F_v) and the maximum chlorophyll fluorescence value (F_m), representing the maximum quantum efficiency of Photosystem II (F_v/F_m), the Performance Index (*PI*), and the number of active reaction centres per unit of leaf surface (RC/CSm). The F_v/F_m ratio is a reliable indicator of the health status of the photosynthetic apparatus and gives information about variations of the photon energy of the photosystem II, while *PI* is a global index of the physiological state [31]. The value of these variables for each pot was obtained as the mean value of measures conducted on three leaves of medium stage (5th and 7th) in the same pot, acquired before the porometer measurements.

The water content of aerial biomass (*AGB_WC*) is a well-known indicator of plant water status. For each pot, *AGB_WC* was calculated from the determination of fresh *(FW)* and dry (*DW*) weights, according Equation (2):

$$AGB\_WC = \frac{FW - DW}{FW} \times 100 \quad (2)$$

To measure *FW* and *DW*, two plants for each pot were sampled every two days during EX2, with the exception of the last date of acquisition, when all plants were collected. The sampled plants were immediately weighed to determine *FW*. Successively, they were dried in a ventilated oven, with a temperature initially set at 60 °C for 20 h, and then at 105 °C until plants reached a constant weight. Finally, they were weighed to determine *DW*.

Measurements carried out for EX1 and EX2 campaigns are summarized in Appendix B.

2.3. Optical and Thermal Indices to Assess the Crop Water Status

Four well-known vegetation indices, calculated from thermal and hyperspectral images, were selected to detect crop water status conditions during the two experiments.

Thermal images were acquired during EX1 and EX2 by means of a thermal infrared camera (TVS-200EX NEC Avio Infrared Technologies Co. Ltd., San Fernando, CA, USA) with a resolution of 640 × 480 pixels, operating in the range of wavelengths between 7.5 and 13 µm. The temperature information within each pixel is expressed in Celsius degree, with a measurement resolution of 0.06 °C, and an accuracy of ±1 °C. The thermal images were acquired during the hottest hours of the day (from 11:00 to 12:30), when the symptoms of crop water stress are likely to be most evident [32]. The thermal camera was kept at a distance of about 40 cm from each pot, with an inclination of approximately 45° with respect to the horizontal plane. The crop emissivity was set to 0.96, according to Sugita et al. [33]. Two artificial references were used in order to normalize the measurements of temperature with respect to the climatic conditions of the greenhouse. These references simulated the behavior of leaves in an optimal hydration and fully open stomata status ("wet" reference, with temperature T_{wet}) and in a dehydration status ("dry" reference, with temperature T_{dry}). The references were made of green paper (paper weight of about 200 g m^{-2}), with rectangular size of about 28 cm^2 [34]. The wet reference was always saturated with distilled water before thermal camera acquisitions, whereas the other reference was kept dry [35]. The references were attached to a background in white polystyrene which was placed behind each pot, so that the camera shots included both crop and references. The thermal images were manually processed, through the software IRT Analyzer 6.0 (Grayess Inc., Bradenton, FL, USA), in order to separate the areas of interest (canopy and "wet" and "dry" references) from areas showing other objects. For each image, a region of interest (RI), not necessarily of fixed size, was selected; the parts of thermal images not including vegetation, such as pot's, soil's or counters' portions, were excluded from the RIs. Afterwards, twenty points within each RI were selected, and the average value of temperature obtained from these points was considered as the canopy temperature for the specific pot (T_{canopy}).

Thus, an index proportional to the leaf conductance for water vapor transfer (I_g) (Equation (3)), and the Crop Water Stress Index (*CWSI*) (Equation (4)), were calculated. Both indices provide information on crop water stress conditions, based on the acquisition of thermal images [11]. Specifically, the I_g values range between 0 (condition of high crop water stress) and ∞ (condition of optimal crop water status), even if maximum values shown in literature do not exceed 10–15 [36]; the *CWSI* values range between 0 (condition of optimal crop water status) and 1 (condition of high crop water stress).

$$I_g = \frac{T_{dry} - T_{canopy}}{T_{canopy} - T_{wet}} \quad (3)$$

$$CWSI = \frac{T_{canopy} - T_{wet}}{T_{dry} - T_{wet}} \quad (4)$$

Hyperspectral images were acquired only during EX2. A hyperspectral imaging line scan sensor, equipped with a Specim V10 spectrometer and a Basler PiA190032gm sensor (operating between 339 and 1094 nm with a wavelength step of 5 nm; DV, Padova, Italy) with active illumination, was mounted on the top of a metal structure. Pots were placed underneath, over a cart moving linearly at constant speed in the direction perpendicular to the line of acquisition in order to acquire an image of the whole pot. A radiometric correction procedure was implemented according to Gowen et al. [37], based on the acquisition of the reflectance spectra of a black target (i.e., a black cover on the sensor) and of a white target (i.e., a white ceramic tile of known reflectance) at the beginning of every acquisition date. Lastly, two optical vegetation indices were derived from the acquired hyperspectral images: the Normalized Difference Vegetation Index (*NDVI*) and the Photochemical Reflectance Index (*PRI*). The *NDVI* index (Equation (5)), which is the most commonly computed vegetation index, is sensitive to the optical properties of the crop photosynthetic pigments [38]. It assumes values ranging from −1 to

1, which describe crop conditions characterized by low to high chlorophyll content, and it is indirectly related to crop health status. The *PRI* index (Equation (6)) is sensitive to the de-epoxidation state of the xanthophyll cycle pigments and to the efficiency of photosynthesis [39]. Several studies demonstrated that the sensitivity of *PRI* to the de-epoxidation state is affected by crop water stress conditions [40]. The *PRI* values range from 0 (healthy canopy) to 1 (stressed canopy).

$$NDVI = \frac{R_{800} - R_{680}}{R_{800} + R_{680}} \quad (5)$$

$$PRI = \frac{R_{570} - R_{530}}{R_{530} + R_{570}} \quad (6)$$

In Equations (5) and (6), R_x is the reflectance at the wavelength x expressed in nm, which is measured through hyperspectral or multispectral sensors.

2.4. Analysis of Variance (ANOVA) and Regression Models

A preliminary ANOVA test was performed to compare the datasets (each of them including reference measurements and spectral indices) collected during the two experiments (EX1 and EX2), in order to verify whether, as expected due to the differences in spinach genotypes, greenhouse microclimatic conditions and nitrogen applications, they shall be treated as independent. After such verification, the two-way ANOVA test was performed to analyze the dependence of thermal and optical indices, as well as of reference water status measurements, on water and nitrogen conditions. For each experiment, data of the considered variable acquired at different times during the experimental period were considered as replicates. The Shapiro–Wilk test was used to verify for each variable the normality of the data sample, while the Bartlett test was used to verify the homogeneity of variance (the non-parametric Fligner–Killeen test was used in alternative for non-normally distributed data samples). The non-parametric Friedman test was performed instead of the ANOVA test only in cases for which the hypothesis of normality and/or homogeneity of variance were not verified.

Variables proven to not be significantly dependent on the nitrogen status were selected. Only for these variables, the correlation matrix between spectral indices and reference measurements was computed. Finally, linear regression models (OLS) between spectral indices and reference measurements were calibrated only for those couples of variables with a correlation coefficient higher than 0.6 in absolute value; moreover, the determination coefficient (R^2) was calculated, and the Fisher test was carried out to assess the significance of the linear regression.

3. Results and Discussion

3.1. Greenhouse Microclimatic Conditions

The climatic conditions in the greenhouse during EX1 and EX2 were quite different. Inside the greenhouse, the global incident radiation (due to external radiation and lighting system) was between 0 and 150 W m^{-2} during EX1, and between 0 and 200 W m^{-2} during EX2. Large differences between indoor and outdoor temperatures occurred during EX1, with a temperature excursion of about 10 °C (indoor and outdoor mean daily temperatures were about 20 °C and 10 °C, respectively). During EX2, the temperature excursion decreased up to 5 °C (indoor and outdoor mean daily temperatures were about 23 °C and 18 °C, respectively) due to the external temperature near the optimal values for the growth of the spinach variety used in EX2 (between 15 °C and 20 °C). Finally, the relative humidity, measured only inside the greenhouse, showed significant differences between EX1 and EX2, the average daily valued being 43% and 58%, respectively, in the two experiments. The illumination and the cooling/heating system inside the greenhouse assured a quite homogeneous environment, avoiding marked differences in climatic conditions that could affect the crop growing.

Figure 2 shows the temporal behavior of the climatic variables hourly measured inside and outside the greenhouse (only the last seven days of each experimental period was reported, to assure a clear

graphical representation), and the daily pattern of the reference evapotranspiration (*ETo*). Figure 2a,c,e refers to EX1, while Figure 2b,d,f to EX2. The hourly temperatures (Figure 2a,b) showed a marked daily cycle during both experimental periods. In particular, the sinusoidal pattern of the temperatures measured inside the greenhouse followed very well the pattern of the external temperatures, with highest values in central hours of the day, and minimum values during the night time. The average daily temperature measured inside the greenhouse was about 18 °C for both EX1 and EX2. The internal global radiation (Figure 2c,d) showed a typical sinusoidal trend with the highest and lowest values around midday and midnight respectively. The radiation inside the greenhouse reached a maximum of approximately 200 W m^{-2} in both EX1 and EX2, while the external radiation reached maximum values of 600 W m^{-2} in EX1 and 800–900 W m^{-2} in EX2. The difference between the internal and external radiation values was likely due to the cover glass decreasing the incoming radiation. The effect of the lamps is clearly visible in Figure 2c,d during early morning and evening hours, when the external radiation was around zero.

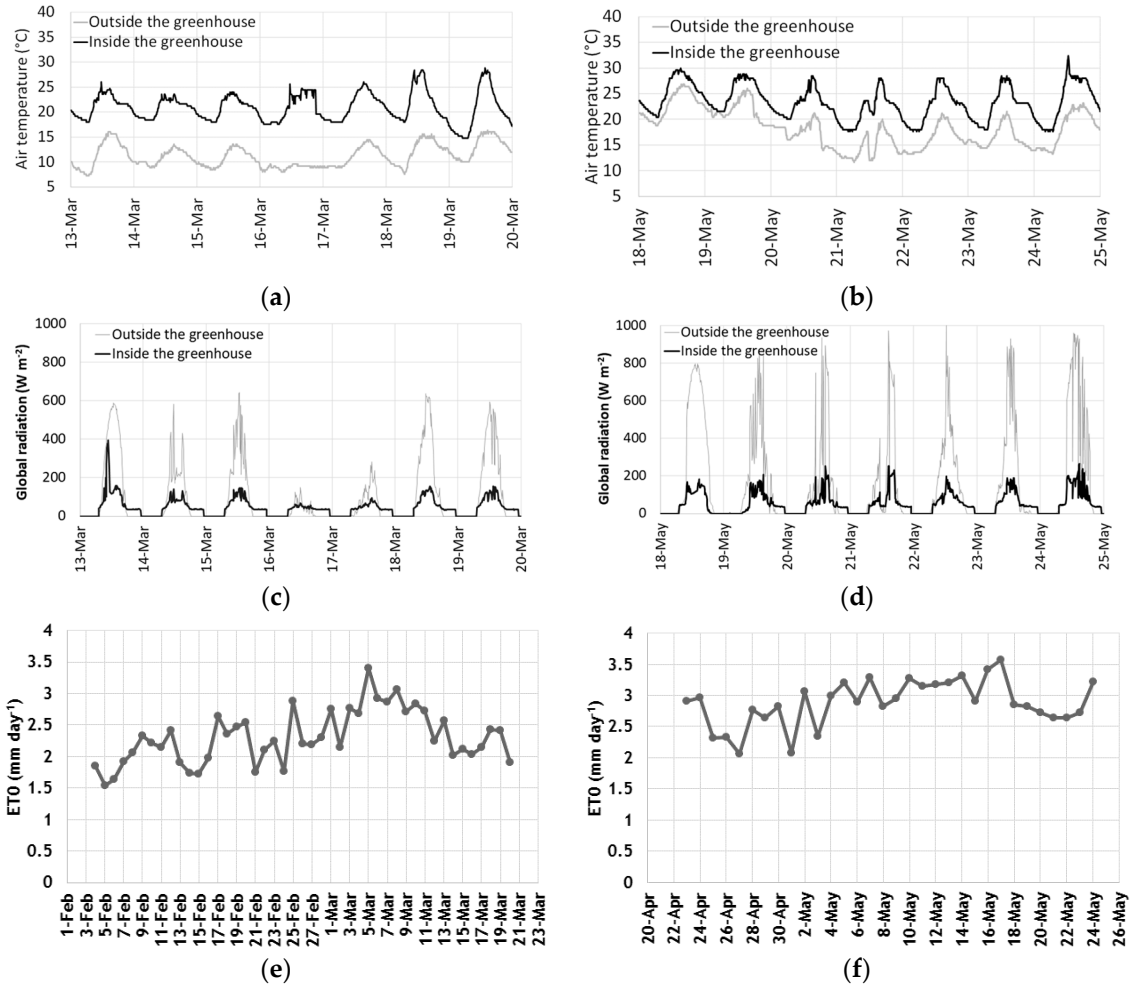

Figure 2. Meteorological variables measured inside and outside the greenhouse: (**a**,**b**) hourly air temperature; (**c**,**d**) hourly global radiation; and (**e**,**f**) daily reference evapotranspiration (ETo).

The daily values of the reference evapotranspiration (*ETo*), calculated according to the Penman–Monteith equation as described in Allen et al. [22], are shown in Figure 2e,f, for the whole periods of EX1 and EX2, respectively. *ETo* trend followed the pattern of the climatic variables. For instance, the highest *ETo* value in EX1 (3.5 mm day^{-1}) was on 5 March, when the daily values of temperature and global radiation (respectively, 35 °C and approximately 650 W m^{-2}) were maximum

in EX1, and the value of relative humidity (below 20%) was minimum in EX1. Overall, *ETo* values ranged between 1.5 and 3.5 mm day^{-1} in EX1 and between 2 and 3.5 mm day^{-1} in EX2.

A more detailed description of the microclimatic conditions in the greenhouse during EX1 and EX2 can be found in Bianchi et al. [4].

3.2. Reference Crop Water Status Measurements

In this section, the behavior of the reference crop water status measurements during EX1 and EX2 is described. Graphics are reported only for *VWC*, whose patterns for the two experiments, highlighting a slope change in the curves, suggest approximate dates at which plant stress began. Analogous patterns (even if in some cases with less evident slope changes) were found for the other variables.

The *VWC* trends during EX1 and EX2 are shown in Figure 3a,b, respectively. For treatment W+, the mean value of *VWC* is almost constant and equal to the field capacity value (0.14 m^3 m^{-3}). Conversely, for treatment W−, the mean value of *VWC* progressively decreases from the day after the interruption of irrigation up to values around 0.06 m^3 m^{-3} and 0.04 m^3 m^{-3} (close to the wilting point, which was found to be 0.05 m^3 m^{-3}) respectively in EX1 and EX2. For W−, a change in the decreasing gradient, which moves from a value of 0.02 m^3 m^{-3} day^{-1} to a value of 0.005 m^3 m^{-3} days^{-1} in both EX1 and EX2, occurs in the last days of the campaigns, precisely on 16 March (for all nitrogen treatments) in EX1, and on 20 May (for N0, N1 and N2) and 21 May (for N3) in EX2. This change in slope can be seen as a change in soil water availability for plants, and thus as a first symptom of plant stress. During the irrigation period, when soil moisture is around the field capacity, the soil water extraction rate is constant under constant environmental conditions. However, when irrigation is interrupted, on some days, the soil water content reaches a critical depletion level, the root water extraction rate begins to decrease (and consequently evapotranspiration falls under the potential rate), and the curve starts to flatten out. The point at which the slope change occurs is the moment at which the plant stress begins. At that point, the soil water content depletion starts to be greater than the RAW (Readily Available Water), which in our experiments seems to be higher than 0.2 TAW as reported in Allen et al. [22] for spinach. As suggested by Bockhold [41], the identification of this point is important for irrigation management.

For treatment W+, the mean value of g_s is around 0.4 cm s^{-1} and 0.6 cm s^{-1}, respectively, for EX1 and EX2. For treatment W−, the mean value of g_s decreases from the day after the interruption of irrigation up to values around 0.1 cm s^{-1} (for all nitrogen treatments) in EX1, and 0.05 cm s^{-1} (for N0 and N3) and 0.2 cm s^{-1} (for N1 and N2) in EX2. Values reached by g_s for treatment W− in EX1 and EX2 are similar to those obtained by Downton et al. [42] on spinach, for a combination of salt and water stresses. Recent studies reported that the g_s in spinach under water stress ranged from 0.2 to 0.7 cm s^{-1} [26]. Moreover, many literature results on horticultural crops revealed a wide variability of g_s values (from 0.01 cm s^{-1} to 0.4 cm s^{-1}) when water stress is occurring [43].

In the case of *AGB_WC*, measured only during EX2, the average value for treatment W+ is about 90% for all the nitrogen treatments. When the treatment W− is considered, *AGB_WC* decreases reaching final values around 84% for all the nitrogen treatments.

The average values of *PI*, F_v/F_m and *Rc*/*Csm* in W+ during both EX1 and EX2 are respectively 2, 0.8 and 2500, while a weak decrease of about 5% with respect to the initial value occurrs in W− for all the indices, regardless of the nitrogen treatment. Jalink and van der Schoor [44] showed that when plants are subjected to abiotic stresses (such as water or nutrient depletion), photochemical activity, measured by *PI*, F_v/F_m and *RC*/*CSm* indices, decreases due to processes of energy dissipation in order to protect the photosynthetic apparatus from deterioration. The literature agrees that it is difficult to define threshold values corresponding to the beginning of stress conditions suitable for all the crops. Many authors, to recognize the beginning of a stress condition, refer to the change in the trend evolution of these variables during the experimental campaign [45].

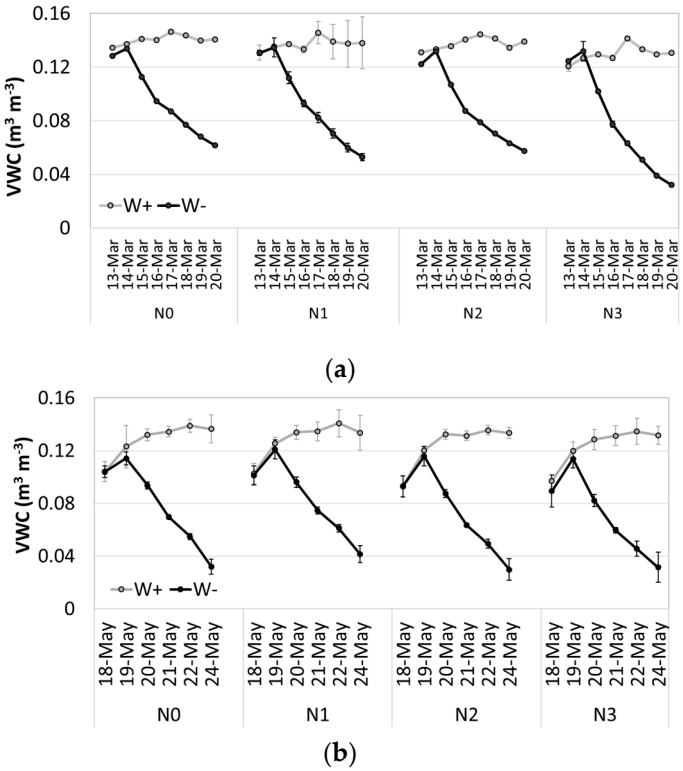

Figure 3. Temporal trends of VWC respectively in: EX1 (**a**); and EX2 (**b**). Points represent the mean value over all the pots characterized by the same water and nitrogen treatments in different times, error bars represent the standard deviations of the pot measurements.

3.3. Crop Water Status and Spectral Indices

In this section, graphics illustrating the temporal trends of thermal and optical indices during EX1 and EX2 are shown. In particular, the graphics report the mean values of indices calculated for all the pots characterized by the same water and nitrogen treatments; the error bars indicate the variability (i.e., standard deviation) of the pot measurements.

The *CWSI* behavior during EX1 and EX2 is shown in Figure 4a,c, respectively. The mean value of *CWSI* varies between 0.2 and 0.4 for treatment W+, while it increases up to about 0.9 for treatment W− in both EX1 and EX2. For W−, a huge increase occurs for N2 and N3, in both EX1 and EX2. An increase of the slope, particularly evident for N2 and N3, occurs on 15–16 March in EX1 and on 20 May in EX2, as a consequence of the beginning of the crop water stress condition (refer to Section 3.2 for a discussion on the slope change in the *VWC* curve).

The I_g trends during EX1 and EX2 are shown in Figure 4b,d, respectively. The mean value of I_g decreases for both W+ and W−, probably due to the plant growth. However, for all nitrogen treatments, the I_g values for W− decrease more rapidly than in the case of W+. Moreover, for W−, a change in the value of the decreasing slope occurs again during 15–16 March for EX1, and during 20–21 May for EX2.

In general, we can observe that both *CWSI* and I_g considerably increase when soil water depletion becomes pronounced. Moreover, *CWSI* and I_g dynamics, similar in both experiments and for all treatments, seem to be strongly related to the patterns of soil water content, leaf water content and stomatal conductance. The maximum value of *CWSI* reached in this study is similar to that obtained over stressed plants of different species by Yu et al. [46]. The literature does not provide a specific value of *CWSI* for an irreversible water stress condition, but it widely agrees that soil water scarcity jeopardizes the physiological response of plants when *CWSI* is greater than 0.85 [47].

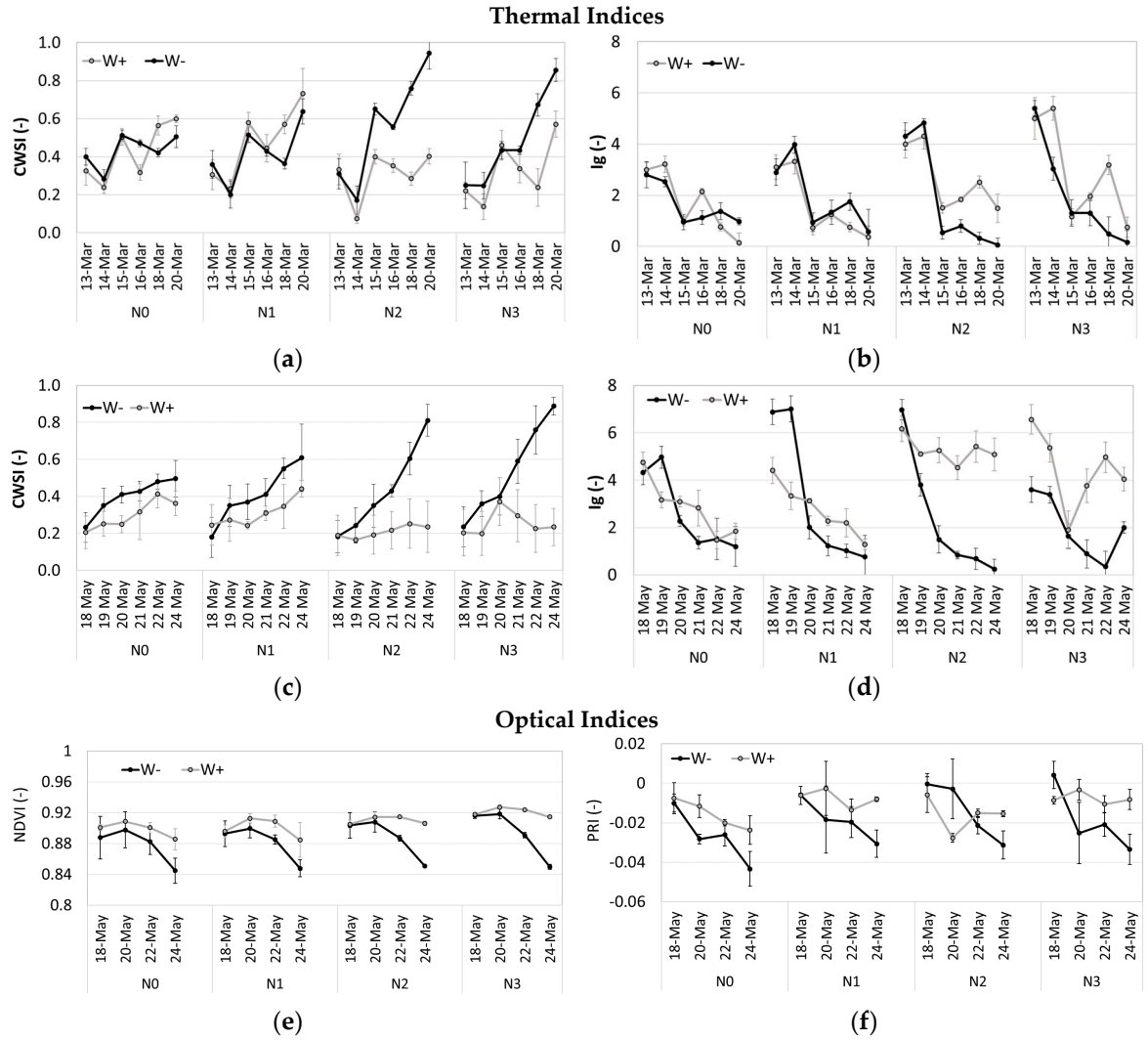

Figure 4. Temporal trend of thermal and optical vegetation indices: *CWSI* and I_g in EX1 (**a**,**b**); and in EX2 (**c**,**d**); and *NDVI* and *PRI* in EX2 (**e**,**f**). Points represent the mean value over all the pots characterized by the same water and nitrogen treatments in different times, error bars represent the standard deviations of the pot measurements.

The trends of optical vegetation indices during EX2 are shown in Figure 4e,f. For all the nitrogen treatments, the *NDVI* value (Figure 4e) is quite constant for W+, while it decreases up to 0.84 for W−. The *PRI* index appears characterized by some variability for both water treatments, but an evident decrease of the index occurs in W− for all the nitrogen levels (Figure 4f). Both vegetation indices show a change in the slope of the temporal pattern on 20 May, according to the behavior of the reference measurements and of the thermal indices. In general, *NDVI* shows a clearer trend and a lower variability in pot measurements when compared to *PRI*. These findings suggest that in the experiment water stress affected the canopy structure more than nitrogen status, probably due to the wide range of water status conditions explored, not commonly found in open field, resulting in a large variation of the leaf area index related to the *NDVI* [19,48].

3.4. The ANOVA Results

The preliminary ANOVA test performed to compare data collected during EX1 and EX2 confirmed that the datasets are different for all the considered variables (reference measurements and spectral indices), with a significance level $p < 0.05$. For that reason, the successive two-way ANOVA test

was separately applied to the dataset of each experiment. In particular, the two-way ANOVA test was carried out for each variable (reference variable or spectral index) of a dataset, to evaluate its dependency on water and nitrogen status. Firstly, the complete dataset including the values of the considered variable measured at all the acquisition times during the experimental period, for all the water and nitrogen treatments, was analyzed. Secondly, in order to consider a range of water status conditions more commonly explored in irrigated agriculture, the ANOVA test was repeated on a dataset composed by the values of the considered variables measured from the beginning of the experiment to the date at which the soil water content is supposed to fall below the RAW (16 March for EX1, and 21 May for EX2). In conclusion, four two-way ANOVA tests were carried out for each variable (two ANOVA tests for the variables measured only in EX2) and, for each dataset separately, the hypotheses of normality and homogeneity of variance were verified.

The two-way ANOVA results obtained considering the complete datasets are shown in Table 2. Only the reference variables F_v/F_m and RC/CSm in EX1 show a significant dependence on the nitrogen status; however, F_v/F_m also depends on the crop water condition. For all the other variables, the behavior is independent from the crop nitrogen status. Among these variables, PI and I_g do not show significant variability due to the irrigation treatment in the case of EX1. The results suggest that PI, among the three fluorescence indices examined, is probably the more dependent on water status, being at the same time independent on the plant nitrogen status. The behavior of F_v/F_m and RC/CSm may be due to the difficulty of these indices to distinguish the effects of multiple stresses (i.e., nitrogen plus water). The $NDVI$ index shows a significant variability due to crop water status, as the PRI index, while it seems to be insensitive to differences in nitrogen status. These results are probably conditioned by the wide range of water status conditions considered. The severe water stress level reached in the experiment EX2 induced effects on the canopy structure more evident than those due to nitrogen stress. In the literature, the dependency of $NDVI$ and PRI on the crop water status is well known, exhibiting a decreasing value of $NDVI$ and PRI in water stressed crops compared to well-irrigated ones [38]. This fact may be explained by the effects of water stress on the xanthophyll pigment cycle production levels [48], determining a decrease of both indices when water stress becomes more evident.

Table 2. Two-way ANOVA test conducted separately for EX1 and EX2; p-values are reported. During each experiment, data acquired in different times are considered as replicates and the entire experimental period is taken into account.

Measurement	Symbol	Irrigation Treatment (W)		Nitrogen Treatment (N)	
		EX1	EX2	EX1	EX2
Reference Variables	VWC	<0.05 *	<0.05 *	ns *	ns *
	g_s	<0.001	<0.05 *	ns	ns *
	F_m/F_v	<0.1	<0.1	<0.001	ns
	PI	ns *	<0.05 *	ns *	ns *
	RC/C_{sm}	ns	ns	<0.001	ns
	AGB_WC	nd	<0.05	nd	ns
Vegetation Indices	$CWSI$	<0.1	<0.05 *	ns	ns *
	I_g	ns *	<0.05 *	ns *	ns *
	$NDVI$	nd	<0.01	nd	ns
	PRI	nd	<0.1	nd	ns

nd = not determined; ns = not significant; * = Friedman test.

The two-way ANOVA test was repeated considering data monitored from the beginning of the experiments to 16 March for EX1 and 21 May for EX2. Results show that reference variables VWC and g_s maintain their independence from the nitrogen treatment in both the experimental campaigns. The same result is found for the thermal indices $CWSI$ and I_g. All fluorescence indices, F_v/F_m, RC/CSm, and PI, show a similar behavior, with a variability explained only by the nitrogen status; thus, in the limited range of soil water content considered, none of them seems to depend on the water treatment.

AGB_WC, measured only in EX2, is found to depend on both water and nitrogen treatments. With respect to optical indices measured in EX2, *NDVI* shows a significant variability due to both the treatments (reduced range of soil water content was considered), while *PRI* is still independent from the nitrogen status.

3.5. Regression Analysis

Correlation matrices of spectral indices with respect to reference measurements were calculated considering the W− datasets, for EX1 and EX2. Due to their irrelevant dependence on crop water status, *Fv*/*Fm* and *RC*/*CSm* were excluded from the analysis. The results for EX1 and EX2 are shown in Table 3. The highest correlations (coefficient greater than 0.60 in absolute value) are found between spectral indices and *VWC*, g_s and *AGB_WC* (except for the I_g index, for which the correlation coefficient with *AGB_WC* is equal to 0.50). Particularly, *CWSI* is negatively correlated with *VWC*, g_s and *AGB_WC*; indeed, the decrease of *VWC* induces a decrease of *AGB_WC*, a stomatal closure (decrease in g_s) with a consequent increase of crop surface temperature and *CWSI*. Conversely, I_g is positively correlated with *VWC*, g_s and *AGB_WC*. *NDVI* and *PRI* are positively correlated with *VWC*, g_s and *AGB_WC*; specifically, crops in water stress conditions are characterized by lower values of *NDVI* and *PRI*. Moreover, *NDVI* and *PRI* show high correlations (coefficient greater than 0.60 in absolute value) with *CWSI* and I_g (the I_g index only with *PRI*). Finally, only *PRI* is found to have high correlation with *PI*.

Table 3. Correlation matrix of spectral indices and reference water status measurements. Results for EX1 (above) and EX2 (below) are reported.

EX1									
		Thermal Indices		**Optical Indices**		**Reference Variables**			
		CWSI	***I_g***	***NDVI***	***PRI***	***VWC***	***g_s***	***PI***	***AGB_WC***
Thermal Indices	*CWSI*	1	−0.84	-	-	−0.79	−0.69	−0.04	-
	I_g		1	-	-	0.75	0.60	0.20	-
Optical Indices	*NDVI*			1	-	-	-	-	-
	PRI				1	-	-	-	-
Reference Variables	*VWC*					1	0.81	0.23	-
	g_s						1	0.37	-
	PI							1	
	AGB_WC								1
EX2									
		Thermal Indices		**Optical Indices**		**Reference Variables**			
		CWSI	***I_g***	***NDVI***	***PRI***	***VWC***	***g_s***	***PI***	***AGB_WC***
Thermal Indices	*CWSI*	1	−0.7	−0.66	−0.7	−0.83	−0.78	−0.22	−0.75
	I_g		1	0.38	0.65	0.75	0.81	0.47	0.50
Optical Indices	*NDVI*			1	0.74	0.80	0.64	0.23	0.95
	PRI				1	0.74	0.82	0.63	0.78
Reference Variables	*VWC*					1	0.90	0.33	0.85
	g_s						1	0.40	0.70
	PI							1	0.29
	AGB_WC								1

The first interesting result obtained is the good correlation between thermal indices and reference measurements for both experiments. This confirms that the two indices, but particularly *CWSI*, can be considered as a proxy of the most commonly adopted (and most costly in terms of time) reference variables for the assessment of crop water stress; thus, they may offer a valid alternative to conventional methods to support the irrigation management. The close correlations found between *CWSI*, *VWC* and g_s agree with what reported in the literature for other crop species [49]. Moreover, *NDVI* and *PRI* also show a good correlation with the reference variables, although in this case measurements were available only for EX2. These results support the potential use of *NDVI* and *PRI* to assess crop water stress, mainly in situations in which the in-field crop variability depends more on differences in water status than in nitrogenous status.

Linear regression models were calibrated for spectral indices with correlation coefficients greater than 0.60 in absolute value with respect to reference variables. The linear regression models for the thermal indices (*CWSI* and I_g) versus the reference variables *VWC*, g_s and *AGB_WC* were calibrated with data collected during EX1 and EX2 separately (Figures 5 and 6, respectively). The linear regression models for the indices *NDVI* and *PRI* versus the reference variables *VWC*, g_s and *AGB_WC* were calibrated with data relative to EX2 (Figure 6). All these regression models, except for the model of I_g versus g_s in EX1, are significant (*p*-value of the Fisher test lower than 0.05).

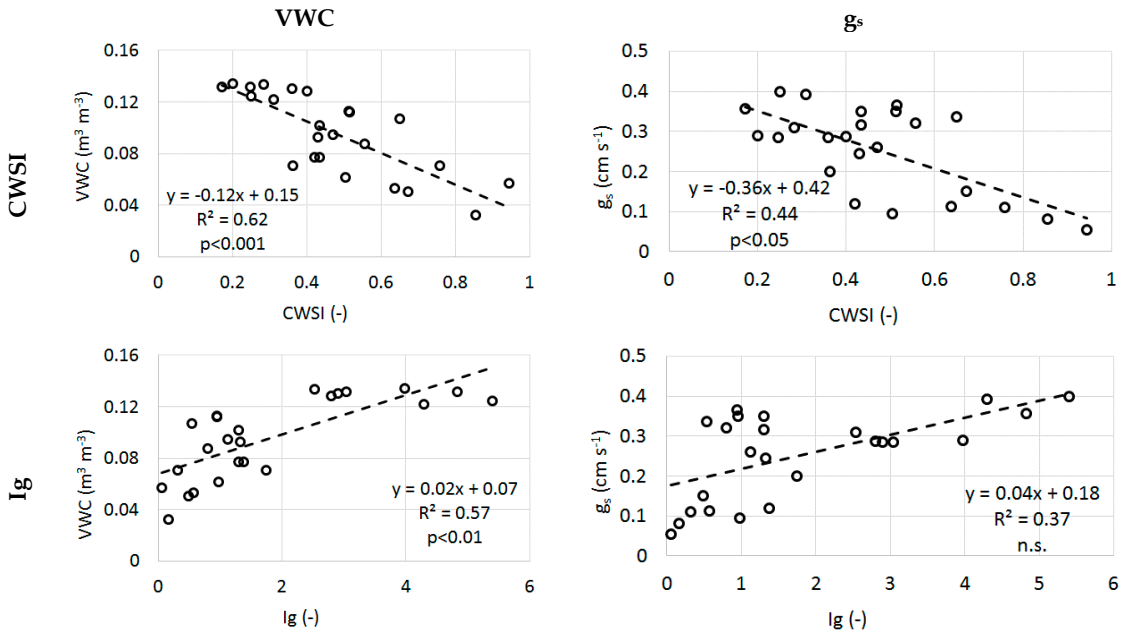

Figure 5. Linear regression models between thermal indices (*CWSI* and I_g) and reference variables (*VWC* and g_s) describing the crop water status. Data are from the EX1 campaign.

In many cases, R^2 is greater than 0.5 (value up to 0.69). The highest R^2 values occur for the regression models between *CWSI* and *VWC* (0.62 in EX1 and 0.69 in EX2), and *NDVI* and *AGB_WC* (0.91), as well as among *PRI*, I_g and g_s (respectively 0.67 and 0.65 in EX2).

The regression model between *CWSI* and *VWC*, for EX1 and EX2, shows high correlation coefficient and very similar parameters in the case of the two experimental campaigns (despite the differences that characterize them), thus proposing itself as a good prediction model for the spinach crop water status. *PRI* and I_g confirmed to be the best indicators for stomatal conductance among the tested indices, according to literature [50,51]; anyway, the parameters of the linear model between I_g and g_s are not so stable for the two campaigns like those between *CWSI* and *VWC*, and in the case of *PRI* and g_s only data acquired in a single campaign are available.

The high determination coefficient found for the regression between *NDVI* and *AGB_WC* confirmed the possibility to use *NDVI* as an indicator for the crop water content in situations when the variability in term of water status conditions is known to be more important with respect to that due to the difference in nitrogen status. In fact, for soil water contents higher than the water stress threshold, the two variables are shown to depend on both stress factors.

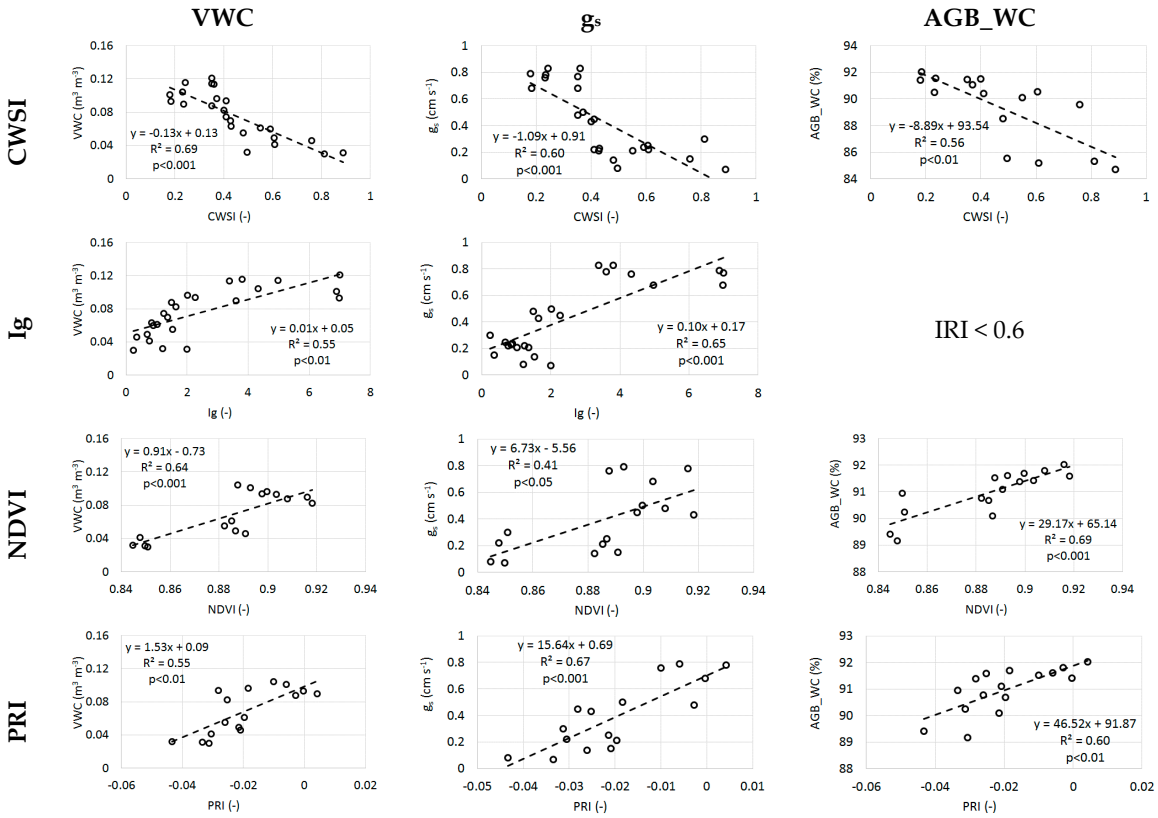

Figure 6. Linear regression models between thermal (*CWSI* and I_g) and optical (*NDVI* and *PRI*) indices, and reference variables (*VWC*, g_s and *AGB_WC*) describing the crop water status. Data are from the EX2 campaign.

4. Conclusive Remarks

The aim of this research was to assess the reliability of indices derived from spectral imaging techniques—thermal indices (I_g and *CWSI*) and optical indices (*NDVI* and *PRI*)—as operational tools to detect and predict water stress in spinach, regardless of the in-field nitrogen condition. To test their ability to reach this goal, two separate experiments (EX1 and EX2) were carried out in a greenhouse, on two spinach varieties (Verdi F1 and SV2157VB), with different microclimatic conditions and under different levels of water and nitrogen application. Common reference variables describing soil and crop water status condition (*VWC*, g_s, fluorescence indices, and *AGB_WC*) were moreover measured.

The ANOVA test allowed to establish the independency of *VWC*, g_s, *CWSI* and I_g from the nitrogen status, whatever the range of soil water content explored. Among the fluorescence indices, only *PI* showed to be independent from the nitrogen status when a soil water content ranging between field capacity and wilting point was taken into account, but its dependence on the nitrogen level became predominant when the water content was limited between field capacity and the water stress threshold. *AGB_WC* and *NDVI* were shown to depend only on soil water status when the wider range of soil water content was considered, and on both water and nitrogen conditions in the case of the more restricted soil water content range.

High correlation coefficients and good linear regression models were found between the spectral indices and the reference variables. In particular, the most significant linear regression models were found between *CWSI* and *VWC* (R^2 of 0.62 and 0.69 in EX1 and EX2), between I_g and g_s (R^2 of 0.57 and 0.60 in EX1 and EX2), between *PRI* and g_s (R^2 of 0.67 in EX2), and between *NDVI* and *AGB_WC* (R^2 of 0.69 in EX2).

In the particular case of spinach grown in greenhouse, this work shows that, for the two investigated varieties, thermal indices derived from high resolution thermal images (especially *CWSI*) can be seen as an adequate operational tool to monitor the crop water status, since no dependence on plant nitrogen conditions was observed. The optical index *PRI* derived from high resolution hyperspectral images showed a good potential to be used for the same purpose, while *NDVI* may be a valuable index for the assessment of severe water stress conditions: in fact, only in this case, the water depletion was shown to induce effects on the canopy more evident than those due to the nitrogen deficiency. Anyway, in the case of optical indices, our findings were based on a single experiment.

The findings of this research may also be useful for open field applications, to derive crop water status information from spectral indices obtained by thermal and multispectral devices mounted on support structures or mobile platforms moving in the field, or on an unmanned aerial vehicle (UAV). In particular, applications could be developed to improve the irrigation scheduling, or to deliver a variable rate irrigation within a single field. Nevertheless, some difficulties to extrapolate the results of this work to open field could be due to the different climatic conditions, sowing density and nitrogen levels affecting the physiological feed-back to the water stress.

Acknowledgments: We wish to thank Andrea Bianchi, Antonia Moreno and Alessandro Ferri for their invaluable help during the experimental campaigns. The project was supported by funds of Department of Agricultural and Environmental Sciences of the University of Milan (Linea A year 2015).

Author Contributions: D.M., M.C., P.M.G., G.C., A.Fe., A.Fa. and B.O. performed the experiments; D.M., M.C., A.Fe. and G.C. analyzed the data; D.M., A.Fa., B.O. wrote the paper.

Conflicts of Interest: The authors declare no conflicts of interest.

Appendix A

Table A1. List of destructive and non-destructive measurements in the experimental campaigns EX1 and EX2.

Type of Measurement	Instrument	Variable	Symbol
Reference measurement			
Non-destructive measurement	Weighing balance	Volumetric Water Content	*VWC*
	Porometer	Stomatal conductance	g_s
	Fluorimeter	Maximum Fluorescence	F_m/F_v
		Performance Index	*PI*
		Active reaction centres	Rc/C_{sm}
Destructive measurement on leaf sample	Weighing balance and oven	Water content of aerial biomass	*AGB_WC*
Stress index			
Non-destructive proximal sensing measurement	Thermal camera	Crop Water Stress Index	*CWSI*
	Hyperspectral apparatus	Stomatal conductance Index	I_g
		Normalized Difference Vegetation Index	*NDVI*
		Photochemical Reflectance Index	*PRI*

Appendix B

EX1							EX2						
March							May						
13	14	15	16	18	20	-	18	19	20	21	22	23	24
T	T	T	T	T	T		T		T		T		T
F	F	F	F	F	F		I	T	I	T	I	T	I
P	P	P	P	P	P		F	P	F	P	F	P	F
					I		P		P		P		P
					L		I		I		I		I
							L		L		L		L

T	Thermal acquisitions
I	Hyperspectral acquisitions
F	Fluorimeter acquisitions
P	Porometer acquisitions
L	Destructive measurements for plant water content determination

Figure A1. Calendar of measurements carried out during the experimental campaigns EX1 and EX2.

References

1. Zarco-Tejada, P.J.; González-Dugo, V.; Berni, J.A. Fluorescence, temperature and narrow-band indices acquired from a UAV platform for water stress detection using a micro-hyperspectral imager and a thermal camera. *Remote Sens. Environ.* **2012**, *117*, 322–337. [CrossRef]
2. Martin, D.L.; Stegman, E.C.; Fereres, E. Irrigation scheduling principles. In *Management of Farm Irrigation Systems*; American Society of Agricultural Engineers: St. Joseph, MI, USA, 1990; pp. 155–203.
3. Masseroni, D.; Facchi, A.; Gandolfi, C. Is soil water potential a reliable variable for irrigation scheduling in the case of peach orchards? *Soil Sci.* **2016**, *181*, 232–240. [CrossRef]
4. Bianchi, A.; Masseroni, D.; Facchi, A. Modelling water requirements of greenhouse spinach for irrigation management purposes. *Hydrol. Res.* **2017**, *48*, 776–788. [CrossRef]
5. Jones, H.G. Application of thermal imaging and infrared sensing in plant physiology and ecophysiology. *Adv. Bot. Res.* **2004**, *41*, 107–163.
6. Costa, J.M.; Grant, O.M.; Chaves, M.M. Thermography to explore plant-environment interactions. *J. Exp. Bot.* **2013**, *64*, 3937–3949. [CrossRef] [PubMed]
7. Idso, S.B.; Jackson, R.D.; Pinter, P.J.; Reginato, R.J.; Hatfield, J.L. Normalizing the stress-degree-day parameter for environmental variability. *Agric. Meteorol.* **1981**, *24*, 45–55. [CrossRef]
8. Panigada, C.; Rossini, M.; Meroni, M.; Cilia, C.; Busetto, L.; Amaducci, S.; Boschetti, M.; Cogliati, S.; Picchi, V.; Pinto, F.; et al. Fluorescence, PRI and canopy temperature for water stress detection in cereal crops. *Int. J. Appl. Earth Obs. Geoinf.* **2014**, *30*, 167–178. [CrossRef]
9. Zia, S.; Romano, G.; Spreer, W.; Sanchez, C.; Cairns, J.; Araus, J.L.; Müller, J. Infrared Thermal Imaging as a Rapid Tool for Identifying Water-Stress Tolerant Maize Genotypes of Different Phenology. *J. Agron. Crop Sci.* **2013**, *199*, 75–84. [CrossRef]
10. Ballester, C.; Jiménez-Bello, M.A.; Castel, J.R.; Intrigliolo, D.S. Usefulness of thermography for plant water stress detection in citrus and persimmon trees. *Agric. For. Meteorol.* **2013**, *168*, 120–129. [CrossRef]
11. Pou, A.; Diago, M.P.; Medrano, H.; Baluja, J.; Tardaguila, J. Validation of thermal indices for water status identification in grapevine. *Agric. Water Manag.* **2014**, *134*, 60–72. [CrossRef]

12. Jones, H.G. Use of thermography for quantitative studies of spatial and temporal variation of stomatal conductance over leaf surfaces. *Plant Cell Environ.* **1999**, *22*, 1043–1055. [CrossRef]
13. Jones, H.G.; Vaughan, R.A. *Remote Sensing of Vegetation: Principles, Techniques, and Application*; Oxford University Press: Oxford, UK, 2010.
14. Liebisch, F.; Kirchgessner, N.; Schneider, D.; Walter, A.; Hund, A. Remote, aerial phenotyping of maize traits with a mobile multi-sensor approach. *Plant Methods* **2015**, *11*, 9. [CrossRef] [PubMed]
15. Corti, M.; Gallina, P.M.; Cavalli, D.; Cabassi, G. Hyperspectral imaging of spinach canopy under combined water and nitrogen stress to estimate biomass, water, and nitrogen content. *Biosyst. Eng.* **2017**, *158*, 38–50. [CrossRef]
16. Zillmann, E.; Graeff, S.; Link, J.; Batchelor, W.D.; Claupein, W. Assessment of cereal nitrogen requirements derived by optical on-the-go sensors on heterogeneous soils. *Agron. J.* **2006**, *98*, 682–690. [CrossRef]
17. Rodriguez, D.; Fitzgerald, G.J.; Belford, R.; Christensen, L.K. Detection of nitrogen deficiency in wheat from spectral reflectance indices and basic crop eco-physiological concepts. *Aust. J. Agric. Res.* **2006**, *57*, 781–789. [CrossRef]
18. Filella, I.; Serrano, L.; Serra, J.; Penuelas, J. Evaluating wheat nitrogen status with canopy reflectance indices and discriminant analysis. *Crop Sci.* **1995**, *35*, 1400–1405. [CrossRef]
19. Eitel, J.U.H.; Long, D.S.; Gessler, P.E.; Hunt, E.R. Combined spectral index to improve ground-based estimates of nitrogen status in dryland wheat. *Agron. J.* **2008**, *100*, 1694–1702. [CrossRef]
20. Römer, C.; Wahabzada, M.; Ballvora, A.; Pinto, F.; Rossini, M.; Panigada, C.; Behmann, J.; Léon, J.; Thurau, C.; Bauckhage, C.; et al. Early drought stress detection in cereals: Simplex volume maximisation for hyperspectral image analysis. *Funct. Plant Biol.* **2012**, *39*, 878–890. [CrossRef]
21. Greenwood, D.J.; Lemaire, G.; Gosse, G.; Cruz, P.; Draycott, A.; Neeteson, J.J. Decline in percentage N of C3 and C4 crops with increasing plant mass. *Ann. Bot.* **1990**, *66*, 425–436. [CrossRef]
22. Allen, R.G.; Pereira, L.S.; Raes, D.; Smith, M. *Crop Evapotranspiration-Guidelines for Computing Crop Water Requirements*; FAO Irrigation and Drainage Paper 56; FAO: Rome, Italy, 1998; Volume 300, p. D05109.
23. Möller, M.; Alchanatis, V.; Cohen, Y.; Meron, M.; Tsipris, J.; Naor, A.; Ostrovsky, V.; Sprintsin, M.; Cohen, S. Use of thermal and visible imagery for estimating crop water status of irrigated grapevine. *J. Exp. Bot.* **2006**, *58*, 827–838. [CrossRef] [PubMed]
24. Clemmens, A.J.; Dedrick, A.R. Irrigation techniques and evaluations. In *Management of Water Use in Agriculture*; Springer: Berlin/Heidelberg, Germany, 1994; pp. 64–103.
25. Digrado, A.; Bachy, A.; Mozaffar, A.; Schoon, N.; Bussotti, F.; Amelynck, C.; Dalcq, A.C.; Fauconnier, M.L.; Aubinet, M.; Heinesch, B.; et al. Long-term measurements of chlorophyll a fluorescence using the JIP-test show that combined abiotic stresses influence the photosynthetic performance of the perennial ryegrass (*Lolium perenne*) in a managed temperate grassland. *Physiol. Plant.* **2017**. [CrossRef] [PubMed]
26. Ors, S.; Suarez, D.L. Spinach biomass yield and physiological response to interactive salinity and water stress. *Agric. Water Manag.* **2017**, *190*, 31–41. [CrossRef]
27. Živčák, M.; Olšovská, K.; Slamka, P.; Galambošová, J.; Rataj, V.; Shao, H.B.; Brestič, M. Application of chlorophyll fluorescence performance indices to assess the wheat photosynthetic functions influenced by nitrogen deficiency. *Plant Soil Environ.* **2014**, *60*, 210–215.
28. Baker, N.R.; Rosenqvist, E. Applications of chlorophyll fluorescence can improve crop production strategies: An examination of future possibilities. *J. Exp. Bot.* **2004**, *55*, 1607–1621. [CrossRef] [PubMed]
29. Maxwell, K.; Johnson, G.N. Chlorophyll fluorescence—A practical guide. *J. Exp. Bot.* **2000**, *51*, 659–668. [CrossRef] [PubMed]
30. Guidi, L.; Calatayud, A. Non-invasive tools to estimate stress-induced changes in photosynthetic performance in plants inhabiting Mediterranean areas. *Environ. Exp. Bot.* **2014**, *103*, 42–52. [CrossRef]
31. Strasser, R.J.; Srivastava, A.; Tsimilli-Michael, M. The fluorescence transient as a tool to characterize and screen photosynthetic samples. In *Probing Photosynthesis: Mechanisms, Regulation and Adaptation*; Taylor and Francis: London, UK, 2000; pp. 445–483.
32. Jones, H.G.; Leinonen, I. Thermal imaging for the study of plant water relations. *J. Agric. Meteorol.* **2003**, *59*, 205–217. [CrossRef]
33. Sugita, M.; Hiyama, T.; Ikukawa, T. Determination of canopy emissivity: How reliable is it? *Agric. For. Meteorol.* **1996**, *81*, 229–239. [CrossRef]
34. Jones, H.G. *Plants and Microclimate*; Cambridge University Press: Cambridge, UK, 1992.

35. Maes, W.H.; Baert, A.; Huete, A.R.; Minchin, P.E.; Snelgar, W.P.; Steppe, K. A new wet reference target method for continuous infrared thermography of vegetations. *Agric. For. Meteorol.* **2016**, *226*, 119–131. [CrossRef]
36. Oerke, E.C.; Mahlein, A.K.; Steiner, U. Proximal sensing of plant diseases. In *Detection and Diagnostics of Plant Pathogens*; Springer: Dordrecht, The Netherlands, 2014; pp. 55–68.
37. Gowen, A.A.; Tiwari, B.K.; Cullen, P.J.; McDonnell, K.; O'Donnell, C.P. Applications of thermal imaging in food quality and safety assessment. *Trends Food Sci. Technol.* **2010**, *21*, 190–200. [CrossRef]
38. Suárez, L.; Zarco-Tejada, P.J.; Sepulcre-Cantó, G.; Pérez-Priego, O.; Miller, J.R.; Jiménez-Muñoz, J.C.; Sobrino, J. Assessing canopy PRI for water stress detection with diurnal airborne imagery. *Remote Sens. Environ.* **2008**, *112*, 560–575. [CrossRef]
39. Gamon, J.A.; Penuelas, J.; Field, C.B. A narrow-waveband spectral index that tracks diurnal changes in photosynthetic efficiency. *Remote Sens. Environ.* **1992**, *41*, 35–44. [CrossRef]
40. Thenot, F.; Méthy, M.; Winkel, T. The Photochemical Reflectance Index (PRI) as a water-stress index. *Int. J. Remote Sens.* **2002**, *23*, 5135–5139. [CrossRef]
41. Bockhold, D.L.; Thompson, A.L.; Sudduth, K.A.; Henggeler, J.C. Irrigation scheduling based on crop canopy temperature for humid environments. *Trans. ASABE* **2011**, *54*, 2021–2028. [CrossRef]
42. Downton, W.J.S.; Grant, W.J.R.; Robinson, S.P. Photosynthetic and stomatal responses of spinach leaves to salt stress. *Plant Physiol.* **1985**, *78*, 85–88. [CrossRef] [PubMed]
43. Kaiser, W.M. Effects of water deficit on photosynthetic capacity. *Physiol. Plant.* **1987**, *71*, 142–149. [CrossRef]
44. Jalink, H.; van der Schoor, R. LED induced chlorophyll fluorescence transient imager for measurements of health and stress status of whole plants. *Acta Hortic.* **2011**, *893*, 307–315. [CrossRef]
45. Quick, W.P.; Chaves, M.M.; Wendler, R.; David, M.; Rodrigues, M.L.; Passaharinho, J.A.; Pereira, J.S.; Adcock, M.D.; Leegood, R.C.; Stitt, M. The effect of water stress on photosynthetic carbon metabolism in four species grown under field conditions. *Plant Cell Environ.* **1992**, *15*, 25–35. [CrossRef]
46. Yu, M.H.; Ding, G.D.; Gao, G.L.; Zhao, Y.Y.; Yan, L.; Sai, K. Using Plant Temperature to Evaluate the Response of Stomatal Conductance to Soil Moisture Deficit. *Forests* **2015**, *6*, 3748–3762. [CrossRef]
47. Leinonen, I.; Jones, H.G. Combining thermal and visible imagery for estimating canopy temperature and identifying plant stress. *J. Exp. Bot.* **2004**, *55*, 1423–1431. [CrossRef] [PubMed]
48. Daughtry, C.S.T.; Walthall, C.L.; Kim, M.S.; De Colstoun, E.B.; McMurtrey, J.E. Estimating corn leaf chlorophyll concentration from leaf and canopy reflectance. *Remote Sens. Environ.* **2000**, *74*, 229–239. [CrossRef]
49. Gonzalez-Dugo, V.; Zarco-Tejada, P.; Nicolás, E.; Nortes, P.A.; Alarcón, J.J.; Intrigliolo, D.S.; Fereres, E. Using high resolution UAV thermal imagery to assess the variability in the water status of five fruit tree species within a commercial orchard. *Precis. Agric.* **2013**, *14*, 660. [CrossRef]
50. Berni, J.A.; Zarco-Tejada, P.J.; Suárez, L.; Fereres, E. Thermal and narrowband multispectral remote sensing for vegetation monitoring from an unmanned aerial vehicle. *IEEE Trans. Geosci. Remote Sens.* **2009**, *47*, 722–738. [CrossRef]
51. Jones, H.G.; Stoll, M.; Santos, T.; Sousa, C.D.; Chaves, M.M.; Grant, O.M. Use of infrared thermography for monitoring stomatal closure in the field: Application to grapevine. *J. Exp. Bot.* **2002**, *53*, 2249–2260. [CrossRef] [PubMed]

© 2017 by the authors. Licensee MDPI, Basel, Switzerland. This article is an open access article distributed under the terms and conditions of the Creative Commons Attribution (CC BY) license (http://creativecommons.org/licenses/by/4.0/).